

HIGH-SENSITIVITY AND SELECTIVITY DETECTION OF PERMANGANATE IONS BASED ON PIG LIVER-BASED CARBON QUANTUM DOTS

TU, Y. J.^{1,2,3} –TIAN, Y. H.⁴ –YANG, Y. L.^{1*}

¹*Faculty of Life Science and Technology, Kunming University of Science and Technology, Yunnan Province 650500, China*

²*Faculty of Environmental Science and Engineering, Kunming University of Science and Technology, Yunnan Province 650500, China*

³*Department of Chemical Science and Technology, Kunming University, Yunnan Province 650214, China*

⁴*School of Metallurgy and Energy Engineering, Kunming University of Science and Technology, Kunming 650500 Yunnan Province, China*

**Corresponding author
e-mail: yilyil8@163.com*

(Received 26th Dec 2018; accepted 3rd May 2019)

Abstract. In this paper, novel fluorescent carbon quantum dots (CQDs) were successfully prepared from pig liver by a simple one-step hydrothermal method. The prepared CQDs were characterized using TEM, XRD, XPS, FT-IR, UV-Vis, and fluorescence spectroscopy. It was found that the CQDs were uniformly distributed in size and exhibited good excitation dependence and excellent photostability. Fluorescent probe was used for detection of permanganate. This paper also studied the fluorescent staining performance of pig liver-based CQDs on four live/dead bacteria to evaluate the low toxicity and application prospects of the CQDs. Under the optimum experimental conditions, the probe showed a good linear range ($R^2 = 0.9967$) and a low detection limit ($0.06 \mu\text{M}$) in the concentration range of $0.1\text{--}50 \mu\text{M}$. The pig liver based-CQDs were proved to be a low toxicity fluorescent dye. These attractive properties indicated that the new CQDs could adapt to various complex pH environments, and thus had extensive prospect and promising application for detection of permanganate in complex environmental samples.

Keywords: *carbon quantum dots, pig liver, bacterial staining, in vivo bio-imaging, MnO_4^-*

Introduction

Manganese is an essential trace element of human body. Too much or too little manganese in the body can cause adverse consequences (Teo and Chen, 2001). Manganese deficiency affects the body's reproductive function, lipid metabolism (da Silva et al., 2006), glucose metabolism (Doroschuk et al., 2004) and immune function (Rask et al., 2015), thus causing mental retardation, dysmotility and balance disorders (Gunter et al., 2010), and skeletal dysfunction (Liang et al., 2006). It can also deform the next generation. The excessive amount of manganese in the body can lead to mental symptoms (Zeng et al., 2017). Therefore, the analysis of manganese in food and environment samples is of important practical significance, and it is highly necessary to monitor the level of manganese in body fluids or environmental samples.

Permanganate is usually oxidable, hazardous explosion chemicals, precursor chemicals, and easy to decompose by heating because they all have the same anions-permanganate ions. Permanganate ion has strong oxidation in acidic solution (acidic

KMnO₄ (potassium permanganate)). It also has certain oxidation in alkaline solution, which is purple red in solution. The oxidation of potassium permanganate can be found in both acidity and alkalinity, but it is more obvious in acidity. In recent years, many methods of manganese detection have been developed, including catalytic kinetic spectrophotometric for the determination of trace manganese, but there are few methods for the determination of permanganate ions. A new fluorescence method for the determination of trace manganese was established (Xu et al., 2004), where the concentration range of MnO₄⁻ is 1.0~2.4 mg/L, the maximum excitation wavelength is 278 nm, the maximum emission wavelength is 616 nm, and the fluorescence intensity and concentration show a good linear relationship by transforming the manganese into MnO₄⁻. The results obtained in this method were satisfactory.

Carbon quantum dots (CQDs) are one of the most popular carbon nanomaterials after fullerene, carbon nanotubes and graphene. They were first discovered in 2004 (Wang and Hu, 2014) when electrophoresis was used to purify single-walled carbon nanotubes. They have attracted great attention due to their excellent optical properties, such as water solubility, chemical inertia, low toxicity, easy functionalization (Li et al., 2012) and high fluorescence intensity, photobleaching resistance and adjustable luminescence color. They have been widely used in detection of metal ions (Lu et al., 2012), anions (Zhao et al., 2011), small organic molecules (Li et al., 2013) and biological molecules (Deng et al., 2014). The method of detecting metal ions or other environmental pollutants using CQDs as a fluorescent probe has received extensive attention due to its excellent sensitivity and selectivity (Clarkson and Magos, 2006). Zhang and Chen (2014) used folic acid as carbon source and nitrogen source to trace mercury ions by nitrogen-doped carbon dots, and the detection limit was 0.23 mol/L.

In this study, fluorescent carbon quantum dots (CQDs) were successfully prepared by simple one-step hydrothermal method using pig liver as a carbon source. Since pig liver is a complex that contains a number of organics and biomolecules including fat, proteins, vitamin B, vitamin C, vitamin E, carbohydrates, cholesterol and minerals, it can be useful for doping of multiple hetero atoms in the CQDs without addition of any additives. In the experiment, we found that MnO₄⁻ could quench the fluorescence of CQDs, and the quenching degree was related to the concentration of MnO₄⁻. To our knowledge, there is no report used CQDs fluorescent probe from pig liver for detection of MnO₄⁻ yet, which provides a new method for sensitive detection of MnO₄⁻. In addition, this method has been successfully applied to detecting MnO₄⁻ in environmental water and soil samples.

Experiment

Instruments and reagents

Pig liver was purchased from a local supermarket in Kunming (Yunnan, China); all analytical reagents, including potassium permanganate (KMnO₄), citric acid, disodium hydrogen phosphate (Na₂HPO₄), FeCl₃•6H₂O and FeCl₂•4H₂O, sodium nitrite, sodium nitrate, KI, NaCl, NaF, copper sulfate, aluminum sulfate, calcium chloride, MnSO₄, BaCl₂, MgCl₂ and sodium sulfide (NaS) were purchased from Shanghai Aladdin Biochemical Technology Co., Ltd. (Shanghai, China); and all solutions were prepared from Milli-Q system ultrapure water (18.2 MΩ.cm, 25 °C).

G9800A fluorospectrophotometer (Agilent Technologies, USA) was used to determine the fluorescence spectrum and its intensity; UV-2600 spectrophotometer

(Shimadzu, Japan) was used to determine UV spectra; Tecnai G2 F30S-Twin high resolution field emission transmission electron microscope (FEI, Netherlands) was used to detect the particle size and morphology of fluorescent quantum dots; TENSOR 27 Fourier transform infrared spectrometer (Bruker, Germany) was used to determine the infrared spectrum and the structure of the material; D8-advance X-ray powder diffractometer (Bruker, Germany) was used to determine the crystal structure morphology; Thermo Scientific K-Alpha X-ray photoelectron spectrometer (Thermo Fisher Scientific Inc. U.S.A.) was used to analyze the elemental composition ratio and chemical oxidation state; XH-B vortex instrument (Shanghai Hanuo Instrument Co., Ltd., China) was used for vortex mixing; and 80-2 high speed centrifuge (Shanghai Surgical Instrument Factory, China) was used for centrifugal filtration.

Preparation of pig liver-based CQDs

The pig liver was dried naturally at room temperature and grinded into powders in a mortar. The CQDs of pig liver were prepared by simple hydrothermal method using pig liver powder as carbon source. Five grams of pig liver powder was dispersed in 150 mL deionized water. Then, the mixture was transferred into a high-pressure autoclave (200 mL) lined with polytetrafluoroethylene (PTFE), heated at 180 °C for 10 h, cooled naturally to room temperature, and centrifuged at 13,000 rpm for 20 min to obtain bright yellow solution, and filtered to remove insoluble substances. In order to obtain pure pig liver-based CQDs, the solution was filtered by 0.22 µm membrane. Finally, the obtained pig liver CQDs were stored at 4 °C for further use. Compared with other synthetic methods, the hydrothermal synthesis of pig liver CQDs is simpler and more feasible. In addition, pig liver as raw material for synthesis is cheap and easily available, and this method is greener and more environmentally friendly.

Fluorescence quenching test for permanganate

Typically, 50 µL of prepared pig liver-based CQDs solution and 1 mL of pH 7.0 citric acid-disodium hydrogen phosphate buffer solution mixed and diluted to 3.0 mL with deionized water were placed in a 10 mL glass centrifuge tube. Then, 2mL permanganate solution or sample with a different concentration was added to the centrifuge tube and the vortex was mixed with 30 s. After 3 min, the fluorescence intensity was measured at excitation wavelength 278 nm and emission wavelength 616 nm on the fluorescence spectrophotometer, and the fluorescence intensity was recorded. The slit width of excitation and emission was 5 nm. In order to evaluate the effect of coexisting interfering substances on the fluorescence intensity of pig liver-based CQDs and the selectivity of permanganate and other substances or ions (including $\text{FeCl}_3 \cdot 6\text{H}_2\text{O}$ and $\text{FeCl}_2 \cdot 4\text{H}_2\text{O}$, sodium nitrite, sodium nitrate, KI, NaCl, NaF, copper sulfate, aluminum sulfate, calcium chloride, MnSO_4 , BaCl_2 , MgCl_2 and sodium sulfide), the fluorescence quenching test was carried out under the same experimental conditions. The schematic diagram of detection of MnO_4^- with pig liver-based CQDs was shown in *Figure 1*.

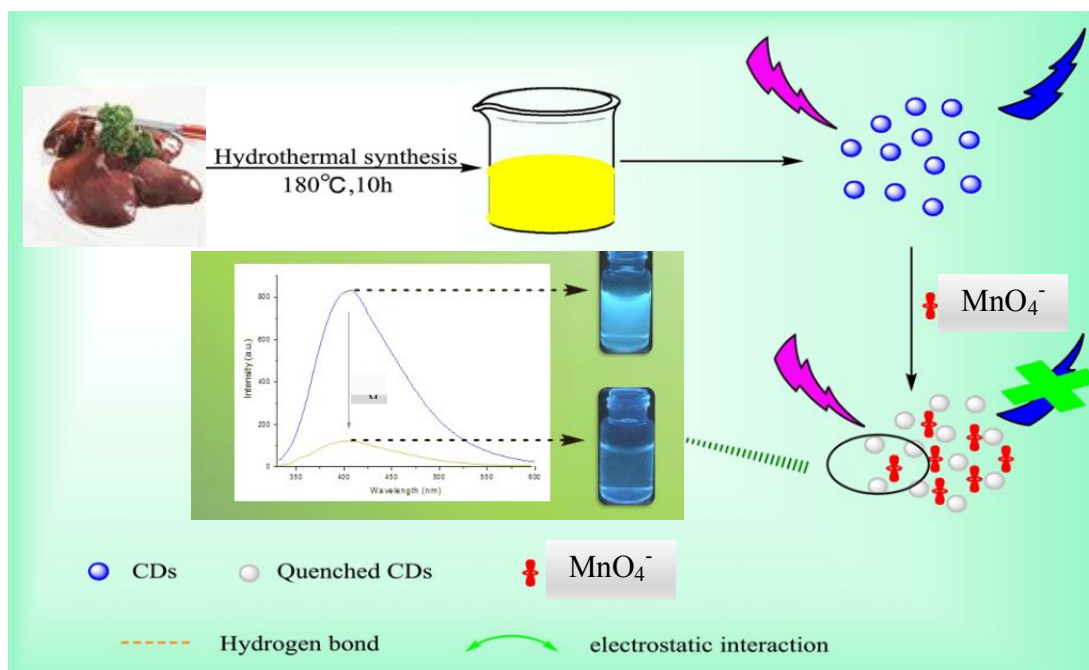


Figure 1. Processing diagram for the synthesis and application of CQDs

Collection and pretreatment of environmental samples

In this study, water samples were collected directly from our laboratory, Laoyuhe Lake and the domestic wastewater of the community next to a school. All water samples were filtered by simple centrifugal filtration to remove solid particles and suspended solids and then by 0.22 μm microporous membrane, and stored at 4 $^{\circ}\text{C}$. The permanganate ion was added to the samples at a concentration of 0.01 mg/mL for spiked fluorescence analysis.

Soil samples were collected from the road outside the school after rain and dried under suitable environmental conditions (final moisture content 0.32%). One milliliter of methanol solution containing different concentrations of permanganate ions was added to 200 mg soil, mixed for 1 h on a 50 rpm shaker, and then allowed to stand overnight at room temperature (RT). On the second morning, the mixture was again vortexed and centrifuged for 2 min at 5,000 rpm and the supernatant was used for fluorescence detection.

Results and discussion

Characterization of the CQDs

The transmission electron microscopy (TEM) technique was used to explore the morphology and particle size distributions of CQDs. As shown in *Figure 2*, the CQDs present high dispersity, uniform spherical shapes, and a size distribution within the range of 3–10 nm and an average diameter of about 5.0 nm. The surface chemistry of CQDs was studied using Fourier transform infrared (FT-IR) spectroscopy. As shown in *Figure 3*, the strong absorption peak at 1469 cm^{-1} reveals the existence of -COOH stretching vibrations; the peak at 1652 cm^{-1} reveals the existence of O=C-NH stretching vibrations; and the absorption peak at 3190 cm^{-1} displays O-H stretching vibrations. As shown in *Figure 4*, the full scan XPS spectra present distinct peaks at

287.3 and 532.7 eV, which are attributed to C1s and O1s, respectively. The result of XPS diagram was consistent with that of FT-IR analysis. Therefore, there should be hydrophilic groups on the surface of pig liver-based CQDs, such as -COOH, -OH, etc., which have good water solubility and broad application prospects.

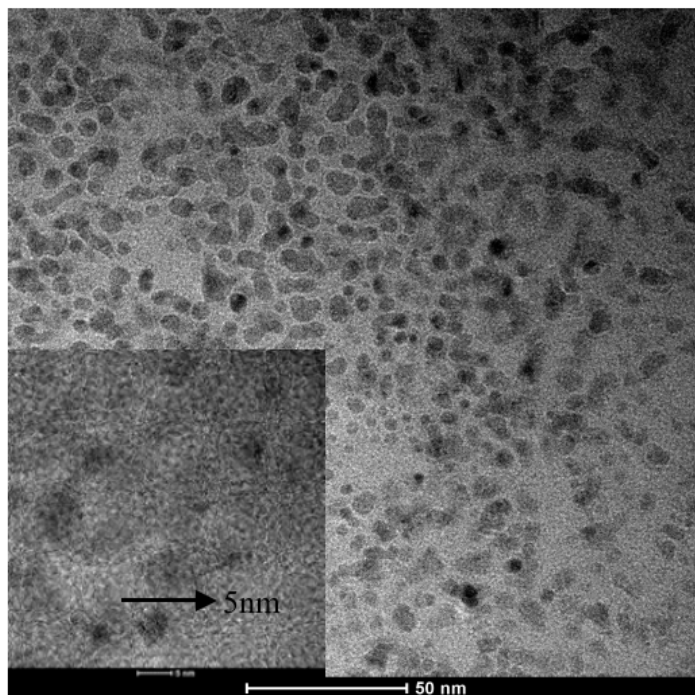


Figure 2. TEM image (inset: HR-TEM image) of the synthesized CQDs

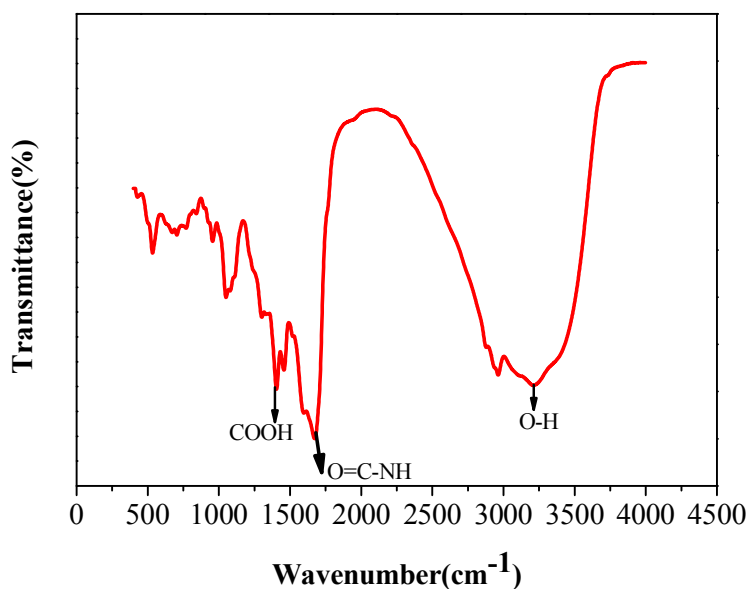


Figure 3. FT-IR spectrum of pig liver-based CQDs

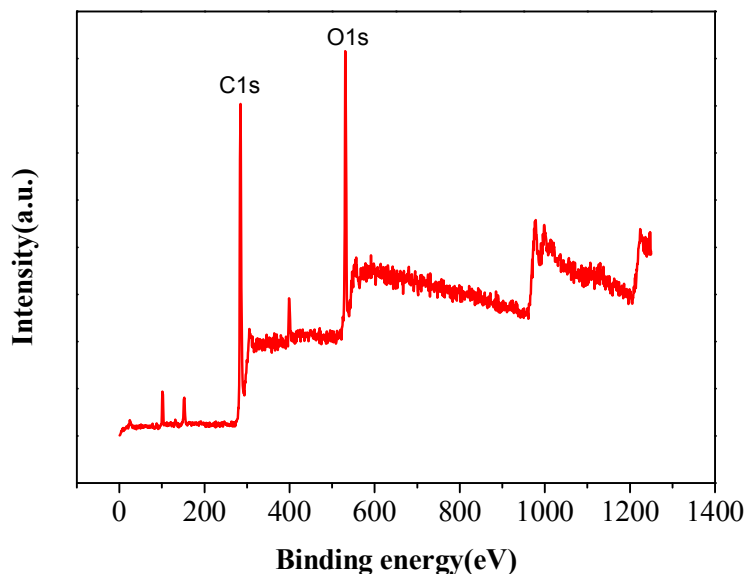


Figure 4. XPS spectra of pig liver-based CQDs

In order to study the optical properties of pig liver-based CQDs, the pig liver-based CQDs were characterized by UV-vis absorption spectrum and fluorescence emission spectrum. The UV-vis absorption spectrum (UV-vis) of pig liver-based CQDs is shown in *Figure 5*. The prepared pig liver-based CQDs had a weak absorption peak around 258 nm and an excitation wavelength of 278 nm at the maximum emission wavelength of 616 nm, as shown in *Figure 6*, a fluorescence spectrum (FS) and an excitation-dependent emission spectrum of pig liver-based CQDs. The results showed that when the excitation wavelength was changed from 300 to 360 nm in increments of 10 nm, the emission peak shifted toward the long wavelength direction.

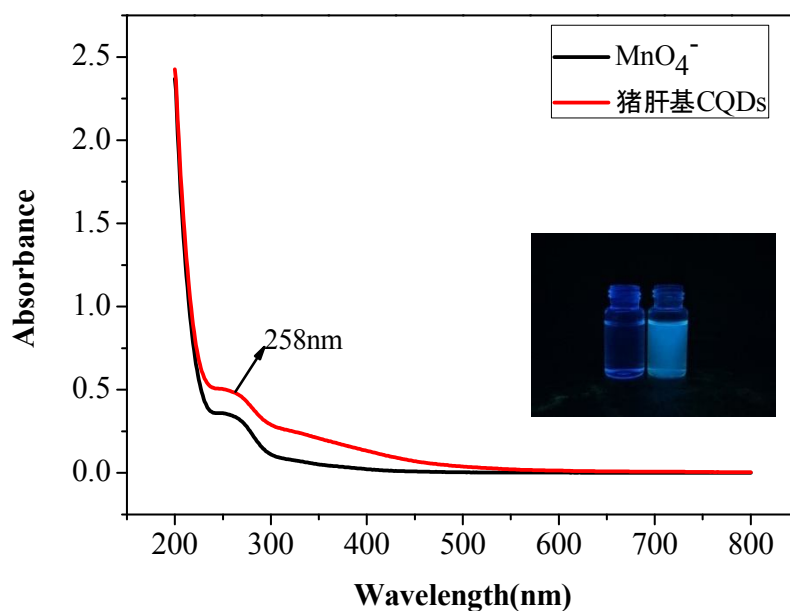


Figure 5. UV-Vis absorption spectra of the synthesized pig liver-based CQDs. (Inset: photographs of pig liver-based CQDs under daylight (left) and UV (365 nm) irradiation (right))

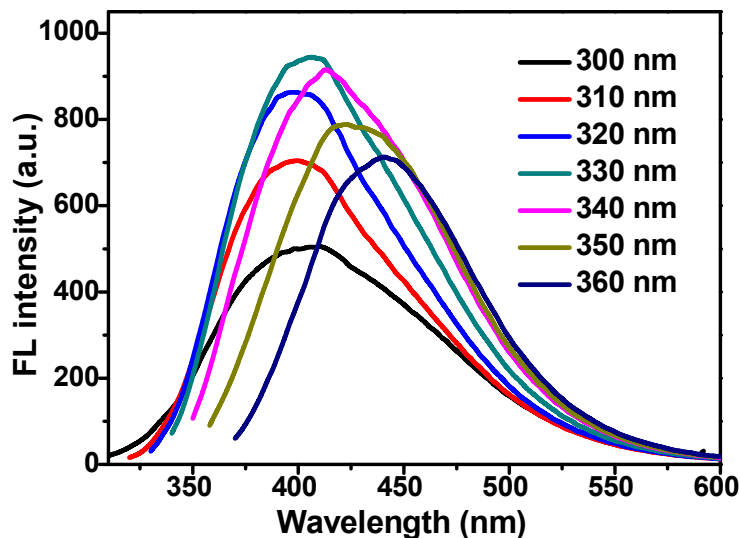
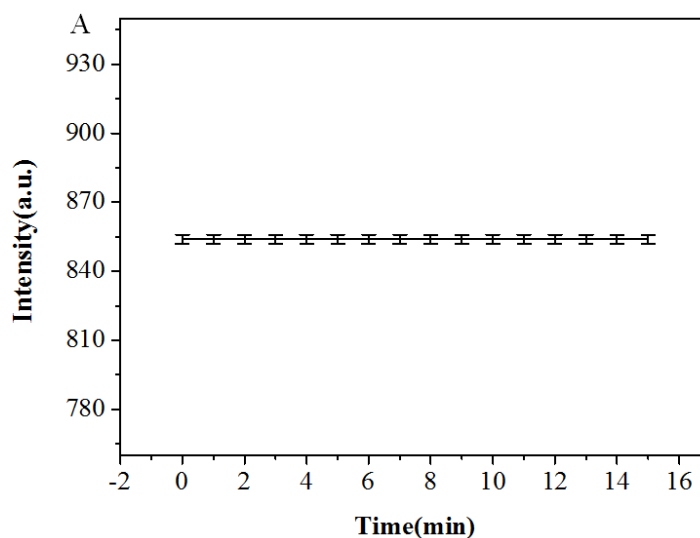


Figure 6. Fluorescence emission spectra of pig liver-based CQDs at different excitation wavelengths

Light stability test of pig liver-based CQDs

In order to study the stability of pig liver-based CQDs in detecting permanganate, the fluorescence intensity of pig liver-based CQDs at different storage time was studied. As shown in *Figure 7A*, the fluorescence intensity of the pig liver based-CQDs is substantially constant. In addition, the reaction time increased while the fluorescence intensity of the experimental system remained constant, indicating that the storage time had no effect on the fluorescence intensity of pig liver-based CQDs. The effects of ionic strength and pH on the fluorescence intensity of pig liver-based CQDs were also studied, as shown in *Figure 7B* and *C*. It is observed from the figures that with the gradual increase of the concentration of NaCl solution, the fluorescence intensity only slightly fluctuated without significant change; the pH of the citric acid-dibasic sodium phosphate buffer changed from 2.0 to 8.0; and the fluorescence intensity of pig liver-based CQDs remain unchanged, this demonstrates that pig liver-based CQDs can be used as fluorescent nanoprobe in any environmental conditions.



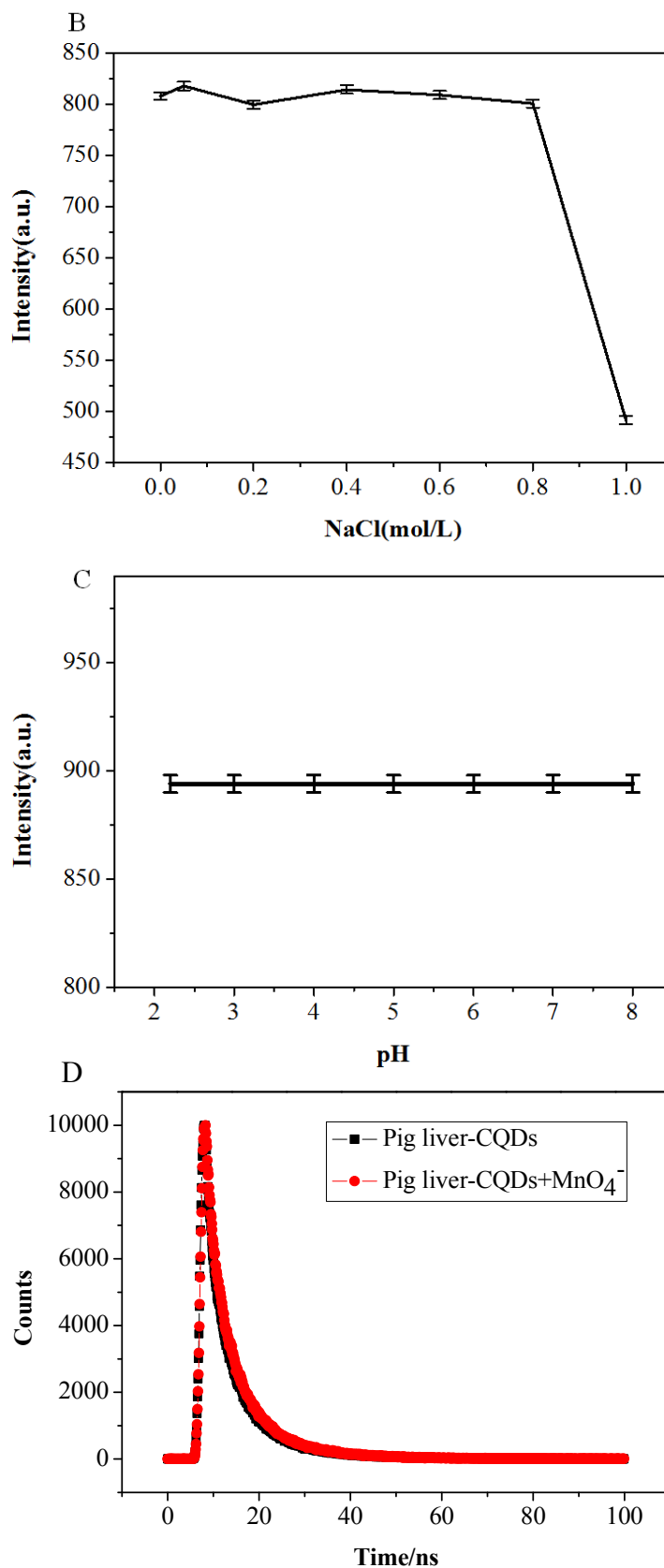


Figure 7. Effects of various conditions on the fluorescence intensity of pig liver-based CQDs: (A) storage time; (B) NaCl concentration; (C) pH; (D) the Fluorescence lifetime decay curve

Selectivity

The selectivity of pig liver based-CQDs was investigated by monitoring the fluorescence intensity of different possible interfering substances such as MnO_4^- , Fe^{3+} , Fe^{2+} , NO_2 , NO_3 , I^- , Cl^- , F^- , Na^+ , K^+ , Cu^{2+} , Al^{3+} , Ca^{2+} , Mn^{2+} , Ba^{2+} , Mg^{2+} and S^{2-} in the presence of different concentrations or ions. As shown in *Figure 8*, only permanganate ion can effectively quench the fluorescence intensity of CQDs in pig liver, while the quenching effect of other possible interfering substances is negligible. The results show that there may be some quenching relationship between pig liver-based CQDs and permanganate ions, which is worthy of further study. Therefore, there is a high selectivity between permanganate ions and pig liver-based CQDs. This demonstrates that pig liver-based CQDs can be used to detect permanganate ions.

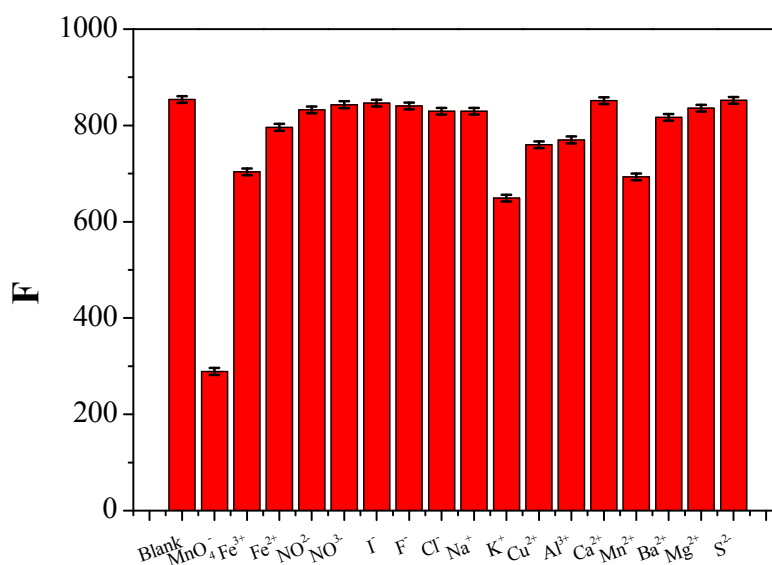


Figure 8. Evaluation of method selectivity against possible interferents

Optimization of experimental conditions

pH affects not only the fluorescence intensity of pig liver-based CQDs, but also the fluorescence quenching effect of permanganate ions on pig liver-based CQDs. Therefore, the effect of pH from 2.2 to 8.0 on the experimental system was investigated. As shown in *Figure 9A*, the fluorescence intensity of pig liver-based CQDs is related to pH. In the range of pH 2.0-7.0, the fluorescence intensity increased gradually and the fluorescence quenching efficiency reached its maximum, but after pH 7.0, the fluorescence intensity decreased gradually. The results show that the fluorescence quenching response of the system is the largest at pH 7.0, according to which pH 7.0 is the optimum pH value of citric acid-disodium hydrogen phosphate buffer.

In order to study the stability of pig liver-based CQDs in detecting permanganate ions, the fluorescence intensity of pig liver-based CQDs in the presence of permanganate ions at the same concentration under different reaction time was studied. As shown in *Figure 9B*, the fluorescence intensity of pig liver based-CQDs decreased sharply within 0-1 min and gradually within 1-10 min, then tended to be stable, and reached the lowest fluorescence intensity in 2 min. Therefore, the reaction time of 2 min was chosen as the optimal fluorescence quenching response time.

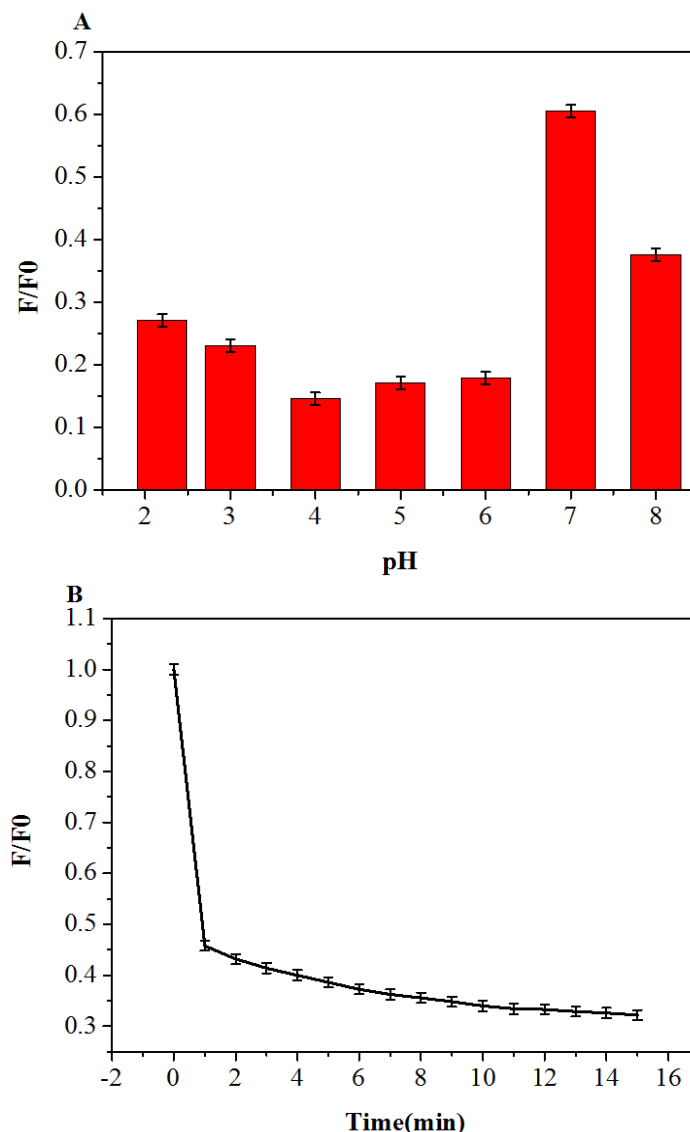


Figure 9. Effect of pH (A) and (B) reaction time on the fluorescence intensity of the pig liver-based CQDs

Method performance study

Under the optimal experimental conditions, the relationship between the fluorescence quenching intensity of pig liver-based CQDs and the concentration of MnO_4^- was studied, and the quantitative analysis method for fluorescence quenching of MnO_4^- was established. As shown in *Figure 10*, the fluorescence intensity of pig liver-based CQDs decreases gradually with the addition of MnO_4^- of different concentrations, and shows regular changes. As shown in *Figure 11*, the ratio of fluorescence intensity of the system was linear with the concentration of MnO_4^- in the range of 0-50 μM both before and after addition of pig liver-based CQDs. The regression equation is $F/F_0 = 0.0151C - 0.0112$ ($R^2 = 0.9967$), where F and F_0 are the fluorescence intensity of pig liver-based CQDs in the presence or absence of MnO_4^- respectively and C is the concentration of MnO_4^- . The detection limit of MnO_4^- was 0.06 μM and the signal-noise ratio was 3(S/N).

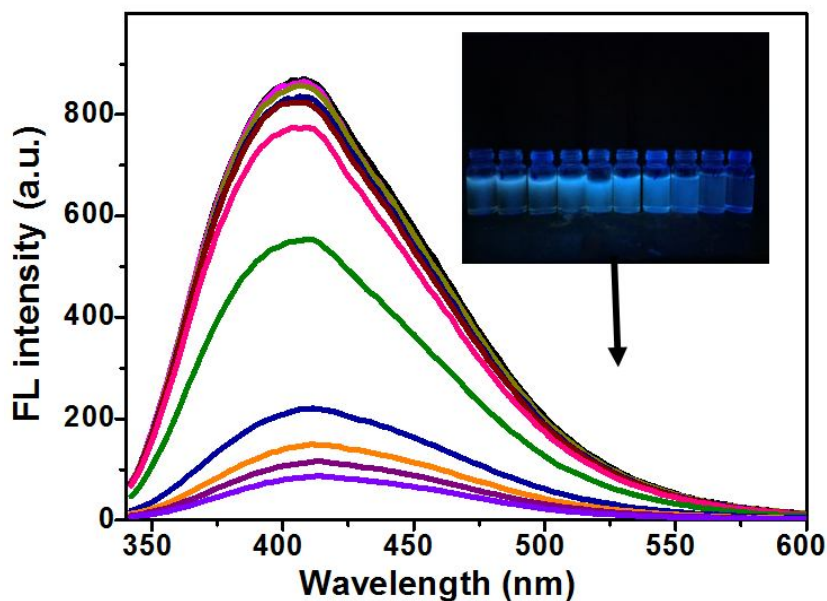


Figure 10. Fluorescence response of pig liver-based CQDs upon addition of different concentrations of MnO_4^- (concentration gradient of pig liver based-CQDs under ultraviolet light)

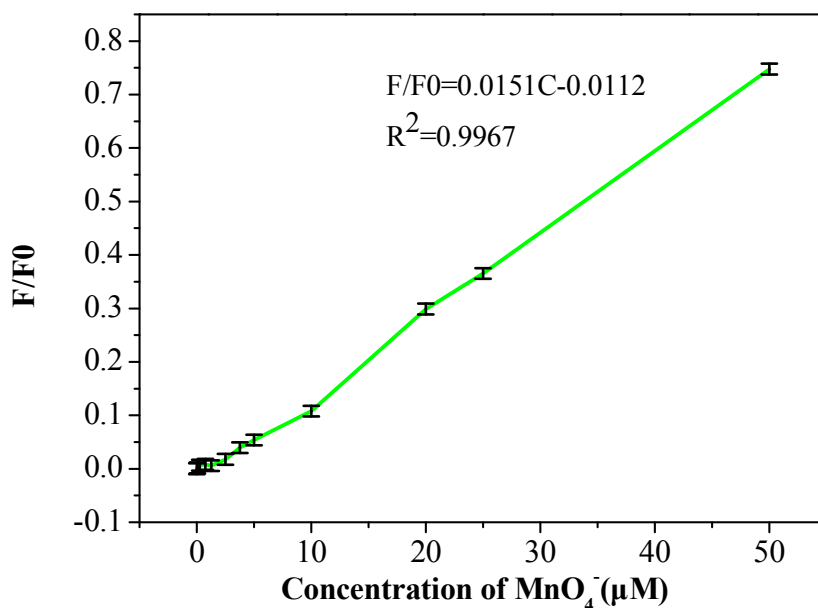


Figure 11. Linear correlation of F_0/F values versus the concentration of MnO_4^- over the range from 0.1 to 50 μM

Possible fluorescence quenching mechanism

In recent years, many sensors have been established based on the fluorescence variation of carbon quantum dots. These sensors were primarily analytes that quenched or increased the fluorescence of the carbon dots (Mariappan et al., 2017). Theoretically, this fluorescence phenomenon is related to different mechanisms. For fluorescence

quenching, the mechanism is usually divided into dynamic quenching and static quenching, caused by the collision between fluorescent materials and quencher and the formation of ground state complexes respectively (Kaviyarasu et al., 2017). In case of dynamic quenching, the Stern-Volmer equation can be used for analysis (Guo et al., 2015) with the following formula:

$$F_0/F = 1 + K_{q\tau_0}[Q] = 1 + K_{SV}[Q]$$

where: F_0 and F indicate the fluorescence intensity before and after the addition of MnO_4^- respectively, K_q is the bimolecular quenching constant, τ_0 is the average lifetime of CQDs, generally 10^{-8} s, K_{SV} is the Stern-Walmer quenching constant, and $[Q]$ was the concentration of MnO_4^- . Therefore, the fluorescence quenching process may be caused by static quenching, i.e. the formation of ground state complexes in the reaction system (Lakowicz, 2006; Sun et al., 2015; Formica et al., 2012). The absorption strength of CQDs increased and the peak shifted to blue after addition of MnO_4^- , indicating that the interaction between MnO_4^- and CQDs produced the ground state complex. According to almost constant fluorescence lifetime, the fluorescence quenching caused by MnO_4^- may be static quenching due to the formation of stable non-fluorescent complexes (Zuo et al., 2016; Sun and Lei, 2017; Wu et al., 2011; Liu et al., 2017, 2014). FT-IR and XPS confirmed the presence of -COOH, -OH, etc. on the surface of CQDs, indicating good water solubility and good application prospect of the synthesized CQDs.

Analysis of MnO_4^- in real samples

The above mentioned environmental water and soil samples were pretreated, and then MnO_4^- in environmental water and soil samples was detected by prepared pig liver-based CQDs. The environmental water samples and soil samples were spiked and recovered using different concentrations of MnO_4^- and pretreated according to the same procedure. As shown in *Table 1*, the recovery of MnO_4^- in water samples is 94.2~102.5% and the relative standard deviations (RSD) of all samples are less than 5.8%. As shown in *Table 2*, the recovery of MnO_4^- in soil samples is 90.5 to 99.5% and the relative standard deviations (RSD) of all samples are below 4.7%. Therefore, this method has the potential for detecting MnO_4^- in environmental water samples and soil samples.

Table 1. Analytical results of MnO_4^- in the water samples ($n = 3$)

Samples	Spiked ($\mu\text{g/mL}$)	Found ($\mu\text{g/mL}$)	Recovery (%)	RSD (% , $n = 3$)
Tap water	0	ND	-	-
	5	4.71	94.2	4.3
	20	19.3	96.5	3.6
Lake water	0	ND	-	-
	5	4.92	98.4	5.8
	20	20.5	102.5	2.5
Waste water	0	ND	-	-
	5	5.10	102.0	5.3
	20	20.05	100.3	4.7

ND = not detected

Table 2. Analytical results of MnO_4^- in the soil samples ($n = 3$)

Samples	Spiked ($\mu\text{g/mL}$)	Found ($\mu\text{g/mL}$)	Recovery (%)	RSD (%, $n = 3$)
Sample 1	0	ND	-	-
	5	4.97	99.5	4.5
	20	18.1	90.5	2.8
Sample 2	0	ND	-	-
	10	9.58	95.8	3.5
	20	18.34	91.7	3.1

ND = not detected

Conclusion

In summary, novel fluorescent CQDs were prepared from pig liver by hydrothermal synthesis method and the fluorescence intensity of CQDs could be quenched by MnO_4^- , so the CQDs were used as nanosensors for the sensitive and selective detection of MnO_4^- in environmental samples. For instance, morphology, particle size, crystal form, chemical element composition and optical properties of the prepared pig liver-based CQDs were characterized by TEM, FT-IR, XPS, UV-Vis and FS. The results showed that it had good stability and fluorescence characteristics. In addition, a good linear relationship was achieved between the fluorescence response of CQDs and the concentration of MnO_4^- in the range from 0.1 to 50 μM . The detection limit was 0.06 μM under optimized conditions. The developed method has been successfully applied to the determination of MnO_4^- in water samples and soils of environmental samples. This method is green, environmental friendly, simple and easy to operate, and shows great potential for application.

REFERENCES

- [1] Bhunia, S. K., Saha, A., Maity, A. R., Ray, S. C., Jana, N. R. (2013): Carbon nanoparticle-based fluorescent bioimaging probes. – *Sci. Rep.* 3: 1473.
- [2] Clarkson, T. W., Magos, L. (2006): The toxicology of mercury and its chemical compounds. – *Crit. Rev. Toxicol.* 36(8): 609-662.
- [3] da Silva, E. G. P., do N. Santos, A. C., Costa, A. C. S., da N. Fortunato, D. M., José, N. M., Korn, M. G. A., dos Santos, W. N. L., Ferreira, S. L. C. (2006): Determination of manganese and zinc in powdered chocolate samples by slurry sampling using sequential multi-element flame atomic absorption spectrometry. – *Microchemical Journal* 82(2): 159-162.
- [4] Deng, X. Y., Li, J. Y., Tan, K. J. (2014): Rapid screening and confirmation of pesticide residues in potato by high-resolution benchtop Q exactive LC-MS. – *Chinese J. Anal. Chem.* 42(4): 579-584.
- [5] Doroschuk, V. O., Lelyushok, S. O., Ishchenko, V. B., Kulichenko, S. A. (2004): Flame atomic absorption determination of manganese (II) in natural water after cloud point extraction. – *Talanta* 64(4): 853-856.
- [6] Formica, M., Fusi, V., Giorgi, L., Micheloni, M. (2012): New fluorescent chemosensors for metal ions in solution. – *Coord. Chem. Rev.* 256 170-192.
- [7] Gunter, T. E., Miller, L. M., Gavin, C. E., Eliseev, R., Salter, J., Buntinas, L., Alexandrov, A., Hammond, S., Gunter, K. K. (2010): Determination of the oxidation states of manganese in brain, liver, and heart mitochondria. – *Journal of Neurochemistry* 88(2): 266-280.

- [8] Guo, Y., Zhang, L., Zhang, S., Yang, Y., Chen, X., Zhang, M. (2015): Fluorescent carbon nanoparticles for the fluorescent detection of metal ions. – *Biosens. Bioelectron.* 63 61-71.
- [9] Hua, X.-W., Bao, Y.-W., Wang, H.-Y., Chen, Z., Wu, F.-G. (2017): Bacteria-derived fluorescent carbon dots for microbial live/dead differentiation. – *Nanoscale* 9: 2150-2161.
- [10] Jones, K. H., Senft, J. A. (1985): An improved method to determine cell viability by simultaneous staining with fluorescein diacetate-propidium iodide. – *J. Histochem. Cytochem.* 33: 77-79.
- [11] Kaviyarasu, K., Kanimozhi, K., Matinise, N., Maria, C. Magdalane, Mola, G. T., Kennedy, J., Maaza, M. (2017): Antiproliferative effects on human lung cell lines A549 activity of cadmium selenide nanoparticles extracted from cytotoxic effects: Investigation of bio-electronic application. – *Mater. Sci. Eng. C.* 76 1012-1025.
- [12] Lakowicz, J. R. (2006): *Principles of Fluorescence Spectroscopy*. 3rd. Ed. – Springer, Singapore.
- [13] Li, H., Kong, W. Q., Liu, J., Liu, N. Y., Huang, H., Liu, Y., Kang, Z. H. (2015): Fluorescent N-doped carbon dots for both cellular imaging and highly-sensitive catechol detection. – *Carbon* 91: 66-75.
- [14] Li, H. T., Kang, Z. H, Liu, Y. et al. (2012): Carbon nanodots: synthesis, properties and applications. – *J. Mater. Chem.* 22(46): 24230-24253.
- [15] Li, J. Z., Wang, N. Y., Tran, T. T. et al. (2013): Electrogenenerated chemiluminescence detection of trace level pentachlorophenol using carbon quantum dots. – *Analyst* 138(7): 2038-2043.
- [16] Li, Z., Yu, H. J., Bian, T., Zhao, Y. F., Zhou, C., Shang, L., Liu, Y. H., Wu, L. Z., Tung, C. H., Zhang, T. R. . (2015): Highly luminescent nitrogen-doped carbon quantum dots as effective fluorescent probes for mercuric and iodide ions. – *Mater. Chem. C* 3: 1922-1928.
- [17] Liang, P., Sang, H., Sun, Z. (2006): Cloud point extraction and graphite furnace atomic absorption spectrometry determination of manganese (II) and iron(III) in water samples. – *Journal of Colloid & Interface Science* 304(2): 486-490.
- [18] Lim, S. Y., Shen, W., Gao, Z. Q. (2015): – *Chem. Soc. Rev.* 44: 362.
- [19] Liu, Y., Zhao, Y., Zhang, Y. (2014): One-step green synthesized fluorescent carbon nanodots from bamboo leaves for copper(II) ion detection. – *Sens. Actuators B* 196: 647-652.
- [20] Liu, Y., Duan, W., Song, W., Liu, J., Ren, C., Wu, J., Liu, D., Chen, H. (2017): Red emission B, N, S-co-doped carbon dots for colorimetric and fluorescent dual mode detection of Fe³⁺ ions in complex biological fluids and living cells. – *ACS Appl. Mat. Interfaces* 9(14): 12663-12672.
- [21] Lu, W., Qin, X., Liu, S. et al. (2012): Economical, green synthesis of fluorescent carbon nanoparticles and their use as probes for sensitive and selective detection of mercury(II) ions. – *Analytical Chemistry* 84(12): 5351-5357.
- [22] Mariappan, A., Kaviyarasu, K., Neyvasagam, K., Ayeshamariam, A., Pandi, P., Palanichamy, R. R., Gopinathan, C., Mola, G. T., Maaza, M. (2017): – *Surf. Interface.* 6 247-255.
- [23] Ming, H., Ma, Z., Liu, Y., Pan, K. M., Yu, H., Wang, F., Kang, Z. H. (2012): Large scale electrochemical synthesis of high quality carbon nanodots and their photocatalytic property. – *Dalton Trans.* 41: 9526-9531.
- [24] Nocker, A., Cheung, C. Y., Camper, A. K. (2006): Comparison of propidium monoazide with ethidium monoazide for differentiation of live vs. dead bacteria by selective removal of DNA from dead cells. – *J. Microbiol. Methods* 67(2): 310-320.
- [25] Rask, J. H., Miner, B. A. Buseck, P. R. (2015): Determination of manganese oxidation states in solids by electron energy-loss spectroscopy. – *Ultramicroscopy* 21(4): 321-326.
- [26] Sun, J., Yang, S. W., Wang, Z. Y., Shen, H., Xu, T., Sun, L. T., Li, H., Chen, W. W., Jiang, X. Y., Ding, G. Q., Kang, Z. H., Xie, X. M., Jiang, M. H. (2015): Ultra-high

- quantum yield of graphene quantum dots: aromatic-nitrogen doping and photoluminescence mechanism. – Part. Part. Syst. Charact. 32: 434-440.
- [27] Sun, X., Lei, Y. (2017): Fluorescent carbon dots and their sensing applications. – Trends in Analytical Chemistry 89 163-180.
- [28] Sun, X., Wang, Y., Lei, Y. (2015): Fluorescence based explosive detection: from mechanisms to sensory materials. – Chem. Soc. Rev. 44 8019-8061.
- [29] Teo, K. C., Chen, J. (2001): Determination of manganese in water samples by flame atomic absorption spectrometry after cloud point extraction. – Analyst 126(4): 534.
- [30] Wang, Y. F., Hu, A. G. (2014): Carbon quantum dots: synthesis, properties and applications. – J. Mater. Chem. C 2(34): 6921-6939.
- [31] Wu, J., Liu, W., Ge, J., Zhang, H., Wang, P. (2011): New sensing mechanisms for design of fluorescent chemosensors emerging in recent years. – Chem. Soc. Rev. 40: 3483-3495.
- [32] Xu, X. Y., Robert, R., Gu, Y. L. et al. (2004): Electrophoretic analysis and purification of fluorescent single-walled carbon nanotube fragments. – J. Am. Chem. Soc. 126(40): 12736-12737.
- [33] Yu, H. J., Shi, R., Zhao, Y. F., Waterhouse, G. I. N., Wu, L. Z., Tung, C. H., Zhang, T. R. (2016): Nitrogen-doped porous carbon nanosheets templated from g-C₃N₄ as metal-free electrocatalysts for efficient oxygen reduction reaction. – Adv. Mater. 28(25): 9454-9477.
- [34] Zeng, C., Qin, P., Lan, L., Wei, H., Wu, W. (2017): Chemical vapor generation coupled with atomic fluorescence spectrometry for the determination of manganese in food samples. – Microchemical Journal 131: 31-35.
- [35] Zhang, R., Chen, W. (2014): Nitrogen-doped carbon quantum dots: facile synthesis and application as a “turn-off” fluorescent probe for detection of Hg²⁺ ions. – Biosensors and Bioelectronics 55: 83-90.
- [36] Zhao, H. X., Liu, L. Q., Liu, Z. D. et al. (2011): Highly selective detection of phosphate in very complicated matrixes with an off-on fluorescent probe of europium-adjusted carbon dots. – Chem. Commun. 47(9): 2604-2606.
- [37] Zuo, P., Lu, X., Sun, Z., Guo, Y., He, H. (2016): A review on syntheses, properties, characterization and bioanalytical applications of fluorescent carbon dots. – Microchim. Acta 183 519-542.